Microfluidic chips for the crystallization of biomacromolecules by counter-diffusion and on-chip crystal X-ray analysis

Kaouthar Dhouib,[a] Chantal Khan Malek,*[b] Wilhelm Pfleging,[c] Bernard Gauthier-Manuel,[b] Roland Duffait,[b] Gaël Thuillier,[b] Rosaria Ferrigno,[d] Lilian Jacquamet,[e] Jeremy Ohana,[e] Jean-Luc Ferrer,[e] Anne Théobald-Dietrich,[a] Richard Giegé,[a] Bernard Lorber[a] and Claude Sauter*[a]

Received 3rd November 2008, Accepted 30th January 2009
First published as an Advance Article on the web 2nd March 2009
DOI: 10.1039/b819362b

Microfluidic devices were designed to perform on micromoles of biological macromolecules and viruses the search and the optimization of crystallization conditions by counter-diffusion, as well as the on-chip analysis of crystals by X-ray diffraction. Chips composed of microchannels were fabricated in poly-dimethylsiloxane (PDMS), poly-methyl-methacrylate (PMMA) and cyclo-olefin-copolymer (COC) by three distinct methods, namely replica casting, laser ablation and hot embossing. The geometry of the channels was chosen to ensure that crystallization occurs in a convection-free environment. The transparency of the materials is compatible with crystal growth monitoring by optical microscopy. The quality of the protein 3D structures derived from on-chip crystal analysis by X-ray diffraction using a synchrotron radiation was used to identify the most appropriate polymers. Altogether the results demonstrate that for a novel biomolecule, all steps from the initial search of crystallization conditions to X-ray diffraction data collection for 3D structure determination can be performed in a single chip.

1. Introduction

X-ray crystallography is a major investigation method in structural biology. In spite of the expanding knowledge of biological crystallogenesis, the production of well-diffracting crystals is frequently the rate-limiting step in the determination of the three-dimensional structure of a biomolecule.[1,2] One reason is that a limited quantity of pure targets (including proteins, nucleic acids, their complexes and viruses) is available. Another one is that usually myriades of assays must be prepared in order to find the crystallant (*i.e.* a salt, an alcohol, a polymer or a mixture of them) in which the best crystals grow. Screening at large scale has become possible owing to the use of robots that can handle micro- or nano-volumes of solution at high speed, which is a necessity in structural genomics and drug design projects to enhance the success of crystallization experiments.[3] Recently a new technological breakthrough happened when microfluidics pushed the limits of miniaturization and parallelization with sample volumes much smaller than those dispensed by robots.[4]

So far there are two major types of microfluidic devices dedicated to biomolecule crystallization. The first one is a block of poly-dimethylsiloxane (PDMS) composed of several polymer layers prepared by multi-layer soft lithography. It contains a multitude of pneumatically actuated valves which serve to fill small parallelepipedic chambers with nanovolumes of biomolecule and reagent solutions and to control their mixing. Crystallization occurs by free interface diffusion (FID)[5] as soon as the latter solutions are brought in contact *via* a short connecting channel[4,6] This type of large scale integrated microfluidic chips has been commercialized since 2003 (Topaz® crystallizer, Fluidigm Corp., CA) and advanced versions provide more control over the crystallization conditions by equilibrating the solutions through a combination of FID and vapour diffusion.[7,8] However, the use of these devices is limited by the evaporation due to the permeability of the polymer, the current cost of the chips and the necessity of an external pressure system to activate the experiments.

The second example is a drop-based or digital microfluidic device also made of PDMS. It uses batch crystallization in nanodroplets, or plugs, formed at regular interval inside a microfluidic channel and separated by an immiscible carrier fluid.[9–11] Biomolecule, buffer, and crystallant solutions are mixed at the junction of independent microfluidic channels. Composition and volume of the droplets can be varied and the latter are stored off-chip either in glass or in plastic capillary tubes for crystal observation and X-ray analysis.[10,12] Using a similar concept, a phase chip was designed to modulate the volume of the drop by water permeation and so to control crystal nucleation and growth kinetics.[13]

We recently developed a novel microfluidic device to crystallize biomolecules in microchannels by counter-diffusion (CD).

[a]*Architecture et réactivité de l'ARN, Université de Strasbourg, CNRS, IBMC, 15 rue René Descartes, F-67084 Strasbourg, France. E-mail: c.sauter@ibmc.u-strasbg.fr*
[b]*FEMTO-Innovation /FEMTO-ST, UMR CNRS 6174 and CTMN, 32 avenue de l'observatoire, F-25044 Besançon, France. E-mail: chantal.khanmalek@femto-st.fr*
[c]*Institute for Materials Research I, Forschungszentrum Karlsruhe, P.O. Box 3640, D-76021, Karlsruhe, Germany*
[d]*Lyon Institute of Nanotechnology, INL, CNRS UMR5270, Université de Lyon, F-69003 Lyon, France and Université Lyon 1, F-69622 Villeurbanne, France*
[e]*Groupe Synchrotron, Institut de Biologie Structurale, CEA, CNRS, Université Joseph Fourier, 41 rue Jules Horowitz, F-38027 Grenoble Cedex 1, France*

This efficient crystallization method,[14] initially implemented in glass capillaries,[15,16] is compatible with direct analysis of crystals by X-ray diffraction[17] and our first results showed that microfluidics is ideal for setting up such kind of experiments in parallel screening on minimal samples volumes.[18,19] Here we report on the manufacturing techniques used to produce four such chips either in PDMS, in poly-methyl-methacrylate (PMMA) or in cyclo-olefin-copolymer (COC). We also discuss important practical aspects, such as solution filling, chip handling, crystal growth monitoring and material X-ray scattering background. Crystals of two proteins grown in these chips were analyzed on-chip by X-ray diffraction on a synchrotron source. The derived protein structures contribute to define the characteristics of a chip in which all steps from initial search of crystallization conditions to optimized crystal growth and 3D structure analysis can be performed.

2. Design and manufacture of microfluidic devices

All chips were designed for equilibrating biomolecule and crystallant solutions according to the principle of counter-diffusion. Therefore, the solution containing the biomolecule must be contained in a long chamber with a small diameter (like a capillary tube or a microchannel). The crystallant (*i.e.* the reagent that will decrease the solubility of the biomolecule and bring it to a supersaturated state) enters this chamber from one side and diffuses gradually across the biomolecule solution. When the concentrations of the compounds are sufficient, the biomolecule becomes supersaturated and may start to crystallize.

The layout of all chips consists of a set of eight parallel microfluidic crystallization channels arranged in a tree-like network on a plane substrate (Fig. 1A). Each channel with a length of 1.5 cm and a 100 × 100 μm² section contains a total volume of about ~150 nl biomolecule solution. Four chips with the same geometry were fabricated in various materials using three manufacturing routes, two methods based on micromoulding using either replica moulding (casting) or hot-embossing, and an alternative method consisting of a one-step laser-based direct manufacturing.

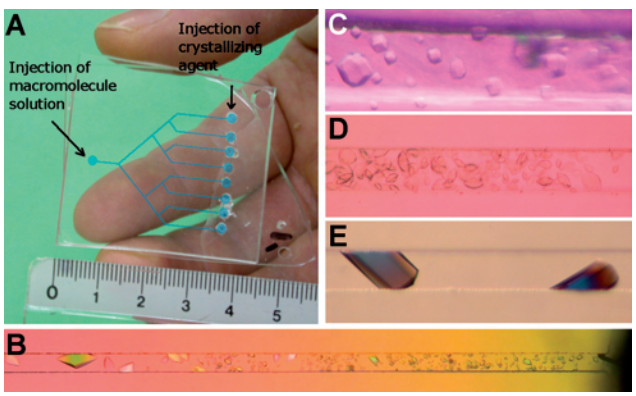

Fig. 1 A chip for biomolecule crystallization by counter-diffusion. (A) Chip geometry: all eight crystallization channels with a section of 100 × 100 μm² are connected through a dichotomic tree-like network on one side to a single inlet or well. First, the sample is filled in this well. Then, the crystallant solution is deposited in the wells at the opposite side of the channels (B) Counter-diffusion in a microfluidic channel: this example of thaumatin crystallization shows typical features of a counter-diffusion experiment. On the right-hand side, close to the reservoir the crystallant concentration is highest and induces a strong amorphous or microcrystalline precipitation. By diffusing through the channel from right to left, it creates a gradient of decreasing biomolecule supersaturation that results in a gradual increase of crystal size. Crystals of: (C) bovine insulin, (D) a plant virus and (E) turkey egg-white lysozyme.

Casting of PDMS chips

PDMS is an inexpensive, rubber-like elastomer with good optical transparency and biocompatibility. It is also the most commonly used material for fast, easy and low-cost prototyping of microfluidic devices in research laboratories. For these reasons, the first prototypes were made of PDMS. Casting was carried out using a two-component rubber temperature vulcanized PDMS (Sylgard 184, Dow Corning) following a standard process based on curing the liquid solution of prepolymer and base (ratio 1/10) on a master.[20] The masters were produced in epoxy-based SU8 negative photoresist patterned by photolithography. The initial thickness of the chip of ~5 mm was subsequently reduced to 1 mm to avoid excessive X-ray absorption. In the first version of the chip, channels were sealed by a layer of PDMS, which was later replaced by two types of thin adhesive films. The first one (ViewSeal™, Greiner BioOne) is a pressure sensitive sealing film made from a polyester/polyolefin laminate coated with a silicone adhesive (130 μm). The second (CrystalClear, Hampton Research) corresponds to Henkel Duck high performance tape (HP260) with a thickness of about 80 μm and an acrylic adhesive. These types of films are widely employed to seal crystallization microplates and were manually applied following manufacturer's recommendation to seal PDMS, PMMA and COC microstructures.

Direct laser machining of PMMA chips

Some PMMA prototypes were fabricated by excimer laser ablation. Structuring was performed with the laser micromachining system Promaster (Optec s.a., France) which operates with an ATLEX-500-SI at a wavelength of 248 nm and a laser pulse length of 5 ns. It is expected that short laser pulses in the ns range significantly reduce thermal contributions to a laser process. The used short pulse excimer generates a raw "flat-top" beam with an intensity fluctuation better than 5%, which is directly applicable without homogenizing devices for a well-defined laser-assisted structuring of polymers. Micro-channels with a depth of 50 μm and a width of 100 μm were fabricated as illustrated in Fig. 2A. The reservoirs (Fig. 2A, left) have a larger depth (250 μm). At the bottom of the reservoir a periodical structure is detected which is caused by the scanning of the laser beam during patterning. A laser beam with a circular aperture of 100 μm was used for the generation of the micro-channels (Fig. 2A, right). Using the excimer laser it took 13 min to produce a prototype.

CO_2-laser processing was performed with the laser system "Firestar v40" (Synrad Inc., USA) operating in continuous mode at 10.6 μm. The beam intensity distribution is Gaussian with a high beam quality. PMMA was patterned using a laser power in the range of 0.2 to 2 W. The processing speed ranged from 10 to 100 mm s^{-1}. The parameters (focus position and line energy,

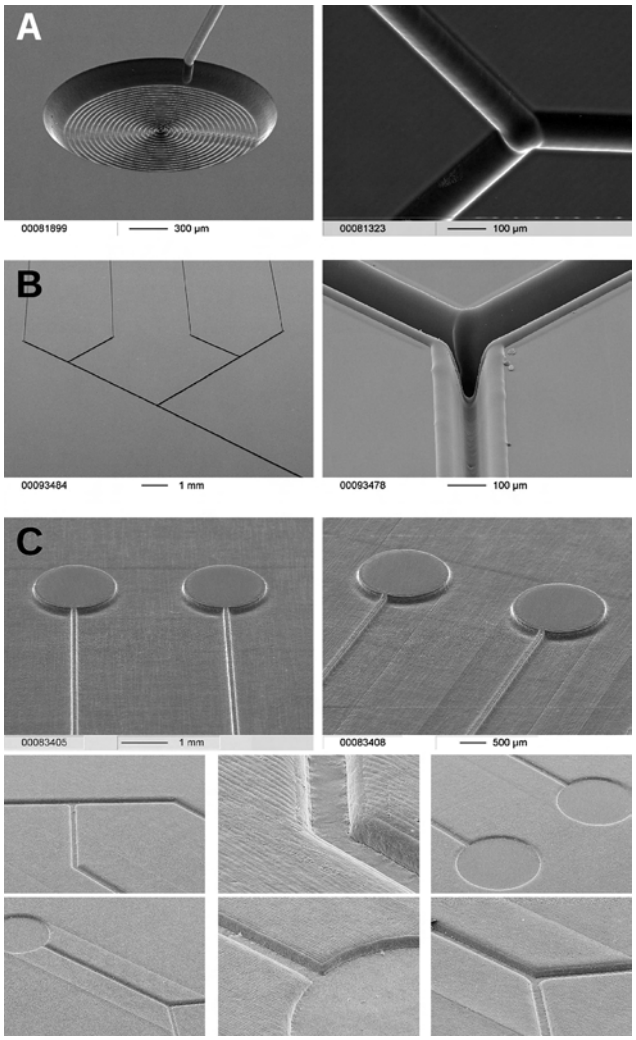

Fig. 2 Scanning electron microscopy (SEM) images of different mould and chip versions. (A) PMMA prototypes micromachined with excimer laser radiation: reservoir (left, repetition rate 300 Hz) and close-up view of the branching zone of the manifold (right, repetition rate 100 Hz). (B) PMMA prototypes micromachined with CO_2-laser radiation: detail of a portion of the tree-like structure of the channel network (left) and close-up view of an intersection (right). (C) Hot embossing mould and PMMA and COC chips: (top panel) mould insert fabricated by laser-micro-carving (material: stainless steel V4A, laser power 7 W, laser scan velocity 40 mm s^{-1}, scan offset 10 µm) and, on the right, a close-up and rotated view; (middle panel) details of the microfluidic chip made by hot-embossing in PMMA showing from left to right, channels with split and bend, close-up view of the bend, and two crystallant reservoirs; (bottom panel) details of the microfluidic chip made by hot-embossing in COC showing, from the left to the right, a reservoir for biomolecule to be crystallized, close-up view of the reservoir, and of channel split.

i.e. ratio of laser power to scanning velocity) for channel widths of 50 up to 200 µm and an aspect ratio of up to 1 were determined. As an example, a focus position of $z = 500$ µm above the surface and a line energy of 19.5 J/m were used to generate fluidic channels with a width of 100 µm (Fig. 2B). Patterning was highly reproducible and average deviation between fabricated and desired cross-section areas of microchannels was better than 3%. It took 3 min to prepare a prototype using the CO_2 laser.

Mould manufacture for hot embossing using laser microcaving

Laser microcaving was performed using a solid state laser radiation source (Nd:YAG, wavelength 1064 nm) with laser powers of $P_L = 1$–10 W in continuous wave mode. The steel substrate used to produce the mould is locally heated up by laser radiation, leading to a temperature rise above the melting temperature. In combination with oxygen as processing gas laser-induced oxidation of the melt occurs. Under special conditions the mechanical tensions inside the oxide layer reach a critical value, and the oxide layer lifts off from the bulk material. The Gaussian laser beam is focused onto the sample surface by an objective lens and scanned over the sample surface *via* deflection mirrors at a speed of up to of 2000 mm s^{-1}. Large areas of up to 110 × 110 mm^2 can be treated. During one laser scan the generated ablation depth is between 1 and 20 µm. A surface quality with a roughness of $R_a = 100$ nm can be realized. Volume ablation rate is in the range of 10^5–10^8 μm^3 s^{-1}.

Hot embossing of PMMA and COC biochips

PMMA is an amorphous polymer widely used in microfluidics. COC, a new generation of polyolefin material based on cyclic and linear olefins, has a number of advantages over other thermoplastic polymers like PMMA, such as reduced water absorption (<0.01%), better chemical resistance to aqueous acids and bases and to most polar solvents. COC is also transparent in the visible and near-UV spectrum, biocompatible and becoming popular in the manufacture of opto-fluidic components. PMMA sheets with a T_g of 105 °C were purchased from Goodfellow. Two grades of Topas® COC 5013 and 6013 (from Ticona now Topas Advanced Polymers GmbH) with $T_g = 130$ °C and 140°C, respectively were purchased as granulates of 1.5 mm diameter. COC 5013 was used for the replication of the chip because its viscosity is lower at high temperature, *i.e.* its melt flow index is higher (48 at 260 °C under 2.16 kg compared to 14 for COC 6013 measured under the same conditions recommended by the manufacturer). For comparison, the melt flow index of PMMA measured at 230 °C and 3.8 kg load following the norm for PMMA [ISO] was 5.5.[21]

Hot embossing was carried out using an in-house built heating press.[20] The embossing tool and the polymers (either in the sheet or granulate form) were first heated at a temperature $T = T_g + 50$ °C. The tool was then brought into contact with the substrate and embossed with a controlled force, typically on the order of 0.1 kN for a tool with a square surface of 40 × 40 mm^2 during several hundreds of seconds so that the polymeric replica conformed to the shape of the mould (Fig. 2C). The tool-substrate assembly was cooled to a temperature $T = T_g - 50$ °C, while the embossing force was still applied. The demoulding took place below this temperature and the embossed polymer substrate was separated from the mould manually. No release layer was used for facilitating the de-embossing process.

3. Crystallization and crystallography experiments

Materials

Bovine insulin, plant thaumatin, turkey egg-white lysozyme, N-(2-acetamido)-2-iminodiacetic acid (ADA), 2-(N-morpholino)

ethanesulfonic acid (MES) and DL-tartaric acid were purchased from Sigma. Hen egg-white lysozyme was from Seikagaku. Turnip yellow mosaic virus (TYMV) was purified as reported.[22] All other chemicals were of ACS grade and used without further purification. All crystallization solutions were prepared with distilled water and filtered before use. PEG-3350, agarose (gelling temperature 28 °C at 1% m/v), and Crystal Clear adhesive tape were from Hampton Research and N-octyl-β-D glucopyranoside (βOG) from Bachem. The critical micellar concentration (CMC) of pure βOG is ~20 mM (0.58% m/v) in water at 22 °C.[45]

Crystallization assays

Protein or virus stock solutions were filtered over 0.22 μm membranes. Solutions used for crystallization assays contained 0.3–1% w/v βOG. Experiments performed in the presence of 0.5% (m/v) agarose sol were set up as following: a 2% (m/v) agarose stock solution was heated at 90 °C during 5 min and cooled to 35 °C before addition to the protein/detergent solution. The final mixture was kept at 35 °C until it was loaded in the channels. The standard procedure for growing crystals in all chips at 20 °C consisted in three steps. First, the sealed wells were opened. Second, 3 μl macromolecular solution was injected (or deposited) with a Hamilton Microliter syringe in the sample well to fill the entire channel arborescence. Third, 2 μl reagent was introduced in each of the 8 crystallizing agent wells with a micropipette. After each filling step, the wells were sealed without delay to prevent the evaporation of well solution and the displacement of channel solution. Following couples of solutions were used to produce crystals: 17 mg mL^{-1} insulin and sodium phosphate 0.5 M pH 10.2; 34–47 mg ml^{-1} thaumatin and 1.5 M sodium tartrate containing 0.1 M ADA pH 6.5; 80–110 mg ml^{-1} turkey lysozyme and 2–4 M NaCl buffered with 0.1 M sodium acetate pH 4.5; 80 mg ml^{-1} hen lysozyme and 0.8 M NaCl containing 30% (m/v) PEG-3350 and 0.1 M sodium acetate pH 4.5; and finally 35–80 $mg.ml^{-1}$ TYMV and 2 M ammonium phosphate with 0.1 M MES pH 3.7.

X-ray analysis

All X-ray analyses were performed at room temperature (T = 20–25°) on the automated synchrotron FIP-BM30A beamline[23,24] of the European Synchrotron Radiation Facility (ESRF, Grenoble France). Material samples and chips were attached onto a microplate that was hold in the beam by the robotic arm for single image or 30–60° oscillation data collection on an ADSC Quantum 315r detector.

The scattering signal of various materials including a 1 mm-thick layer of PDMS and 220–250 μm thick sheets of PMMA, SU8, polypropylene (PP), COC and cyclo-olefin-polymers (COP) (Zeonex 480 or 480R, Zeonor), was measured for an exposure of 30 sec with a sample-to-detector distance of 350 mm. Images were recorded at the wavelengths 0.98 Å and 1.54 Å commonly used in structural biology. Scattering images and radial intensity plots were compared using adxv X-ray image viewer (http://www.scripps.edu/~arvai/adxv.html).

Crystal characterization was performed a week after the beginning of the crystallization assays. Crystals were irradiated inside the chips. In a first set of experiments, thaumatin crystals grown in parallel in PMMA and PDMS chip were compared with a total oscillation range of 40° (ESRF storage ring operating at 200 mA). In a second one, thaumatin crystals grown in COC chip in the presence of agarose gel as well as lysozyme crystals were analyzed with a total oscillation range of 60° (storage ring operating at 50 mA). All analyses were carried out at the selenium edge (wavelength of 0.98 Å), exposure time and angle were adjusted to avoid too many overloaded pixels. Reflections were indexed, processed, and scaled using XDS package[25] and structure factors were generated using the program TRUNCATE from CCP4.[26] Structures were solved by molecular replacement and refined with PHENIX.[27] Thaumatin and hen lysozyme structures contained in the PDB (accession codes 1THW and 1AZF, respectively) were used as search models.

4. Results and discussion

Counter-diffusion in microfluidic environments

Beside sample volume miniaturization, microfluidic systems present a supplementary advantage for crystal growth: channels and chambers with sections below 100 × 100 μm^2 provide convection-free environments. This property was instrumental for the design of the aforementioned FID chip. Indeed, the absence of convection is required in FID to ensure a gentle mixing of biomolecule and crystallant solutions. Thus, it will occur by pure diffusion at the liquid–liquid interface created when the two solutions are brought in contact.

More generally, it was demonstrated that crystals of superior quality can be grown when convection is low or negligible, as it is the case under microgravity,[28] within hydrogels (like agarose or silica)[29] or inside thin capillary tubes. Convection-free environments are also a prerequisite for counter-diffusion. In the absence of convection the crystallant diffuses into the biomolecule solution and generates a concentration gradient inside an elongated crystallization chamber like a cylindrical capillary tube[30] (otherwise both solutions mix by convection and reach quickly the equilibrium.) For this reason CD is the most powerful method for searching and optimizing crystallization conditions.

In the case of FID chips, typical lengths for crystallization chambers are 0.1–1 mm and crystallant concentration will equilibrate rapidly. If one considers Einstein's relation for the mean-square displacement of molecules in solution $<x^2> = 2Dt$ and an average diffusion coefficient for a salt $D = 10^{-5}$ cm^2 s^{-1}, small crystallant molecules will cross a 1 mm chamber in a few minutes and equilibration will be achieved in a few hours. Biomolecules diffuse 1 to 2 orders of magnitude slower than the crystallants (for instance $D = 1.2 \times 10^{-6}$ and 10^{-7} cm^2 $s^{-1}$for lysozyme and a small quasi-spherical plant virus, respectively). In that respect, FID can be seen as a delayed batch experiment in which biomolecule and crystallant solutions mix slowly by diffusion.

In contrast, CD setups require starting conditions far from equilibrium, *i.e.* high crystallant concentration, and much longer crystallization chambers, measuring typically 4–5 cm. The same small molecule will take about 15 days to cross the chamber and, doing so, it will generates a concentration and a related supersaturation gradient. Each single CD experiment is actually characterized by the propagation of a supersaturation wave of gradually

decreasing amplitude that samples a broad range of nucleation and growth conditions[15,31] At the entrance of the chamber a precipitate may form and at the opposite end single crystals may grow. Major experimental prerequisites for such a crystallization experiment, namely a long diffusion path and the absence of convection, are easily met inside a microfluidic channel. Therefore, microfluidic devices are very well adapted for the miniaturization of counter-diffusion experiments[19,32] as it is illustrated below.

Chip design and production

In the first step of this project, several layouts including alignments of isolated channels and comb- or tree-like arrangements of channels have been compared (not shown). The retained design consisting of parallel channels arranged as a dichotomic tree confers two practical advantages (Fig. 1). Firstly, the macromolecular solution can be loaded manually in a single operation through one inlet (the submicroliter sample volume required per individual experiment would be hardly manageable by hand). Then the solution flows simultaneously in the 8 crystallization chambers with a length of 1.5 cm and a section $100 \times 100\ \mu m^2$. Secondly, dead-volume, liquid handling, and sample consumption are minimal. Crystallization chambers are connected with voluminous reservoirs in which the concentrated crystallant solutions are deposited. The volume of a reservoir is typically 10 to 100 times that of the channel to ensure a large excess of crystallant (salt, alcohol or polymer) and create a supersaturation gradient by diffusion. Reservoir solutions can be handled manually or *via* a liquid dispensing system.

Four chips with the same geometry were fabricated in various materials using three manufacturing routes. Two methods are based on micro-moulding, therefore involve the use of a master or mould with *negative* features to produce the parts with the desired *positive* features in a soft elastomer (PDMS) or rigid thermoplastic polymers (PMMA, COC) using respectively replica moulding or hot-embossing in a subsequent replication step. The alternative method involves a one-step laser-based direct manufacturing with neither a mask nor a mould. Advanced laser processing was used in different instances, for generating a metallic mould for hot embossing using micro-caving and for direct patterning of the microfluidic circuit in polymer. The use of lasers for chip manufacture, in particular for microfluidics applications, was the object of recent reviews.[33–35]

The first chip was made of PDMS by soft lithography which is very suitable for fast prototyping. PDMS prototypes showed that crystals could be grown and analyzed in a chip. Although they served to validate the concept, we abandoned them because of several practical limitations explained below. For this reason, chip prototypes with the same geometry were then produced in PMMA and COC by either laser ablation or hot embossing.

UV-laser was applied for micro machining fluidic components in PMMA by photo-ablation ("cold ablation") in the prototyping phase.[36] UV-laser-assisted machining is relatively slow and it cannot be used beyond small series to produce a large number of components at a low cost. On the other hand, infrared (IR) lasers are commercial equipment widespread in industrial applications. Unlike UV laser ablation of polymers, IR laser processing is a purely thermal process. IR laser machining evaporates the substrate material directly by applying heat with the laser beam. CO_2 lasers can provide a cost effective alternative to UV lasers for structuring some polymer substrates. In particular, a CO_2 laser can be used not only for prototyping but also cost-effective production of microstructured components. Prototypes made in PMMA were manufactured by maskless direct-writing using an excimer or a CO_2 laser (Fig. 2A and B).[37]

Hot embossing is a micro-replication technique used to imprint microstructures into a polymer substrate with a mould (Fig. 2C). It exploits the flow of the polymer material heated above its glass transition temperature and compressed between two plates under constant load. In contrast to other more conventional forming processes (extrusion, injection), the hot-embossing process may be performed at temperatures slightly higher than the glass transition temperature of the polymer. It is generally used to manufacture prototypes or small series, whereas the micro-injection process is more adapted to produce micro-components in large batches, *i.e.* mass production. The mould used for this microreplication technique was produced by laser-assisted micro-patterning. The main challenge is to obtain defect free and smooth surfaces during laser processing. Laser-micro-carving[38,39] which can be described as laser-induced oxidation was used to produce the mould in stainless steel V4A. The patterning of metallic surface enables a "clean" patterning process with only a small amount of debris and melt. No release layer was used for facilitating the de-embossing process. The microstructures from the master were fully transferred to the polymer replica with a good fidelity. Fig. 2C shows pictures of details of the hot-embossed biochips in PMMA and COC substrates.

Material constrains in biocrystallization applications

The materials used to manufacture our chips must meet some requirements to facilitate sample loading in the microchannels, crystal growth monitoring and be suitable for on-chip crystal analysis. First all polymers employed here are essentially hydrophobic. *A priori* this is a hindrance for the filling of aqueous solutions in channels by capillarity. We have found that the addition of a small amount of detergent (*e.g.* 0.3–1% w/v of βOG) greatly accelerates the introduction of biomolecule solutions inside PDMS, PMMA and COC. For instance, a 3 μl droplet of aqueous solution with detergent fills the channels within 20–60 s. Detergents are commonly employed in membrane protein crystallization but they are also useful during the crystallization of cytoplasmic, and presumably water soluble, biomolecules to increase their conformational stability and to facilitate the preparation of concentrated samples.[40]

Once the sample is inside the channels, the crystallant solution is deposited in the well located at the other end of each channel and CD starts immediately. Several biomolecules including bovine insulin (6 kDa), turkey egg white lysozyme (14 kDa), the sweet protein thaumatin (22 kDa), and a spherical plant virus (TYMV, 9 MDa) were successfully introduced in the various chips and crystallized in the presence of their respective crystallant (Fig. 1B to E). The distribution pattern of the crystals along the channel is characteristic of CD. As can be seen in Fig. 1B, a precipitate and very small crystals forms on the side of the entry of the crystallant (on the left of the picture) where supersaturation is maximal. The thaumatin crystals are bigger near the opposite end of the channel where supersaturation is

lower. In some cases thaumatin and lysozyme crystals filled completely the channel.

Material transparency in visible light is another necessary condition to observe and monitor crystal growth. PDMS, PMMA and COC are colourless and show no birefringence in polarized light (Fig. 1). The rigidity and air-tightness of PMMA and COC are advantages over the flexibility and permeability of PDMS. They provide a better control over crystallization conditions and improve the stability of crystals since the latter contain on average 35 to 80% solvent, are fragile and very sensitive to dehydration.

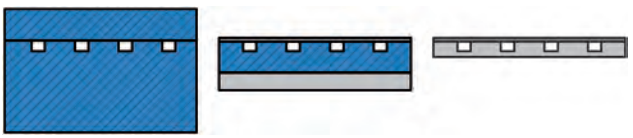

Fig. 3 Evolution of chip thickness and design for on-chip crystal characterization. (Left) First chips consisting in a PDMS layer with channels closed by a PDMS cover. Overall thickness (5 to 6 mm) is incompatible with X-ray analysis. (Center) Second version consisting of a 1 mm thick PDMS layer and a PMMA foil of 250 μm. Channels are closed with a thin tape or adhesive film. This configuration permitted the on-chip characterization of a thaumatin crystal (see Fig. 6A). (Right) Third version made of PMMA or COC that are more rigid than PDMS and interfer less with X-ray (see Fig. 4 and 5).

Sample dehydration and mechanical stress, as well as solution movements and crystal destruction during handling are avoided.

We noticed that sample loading varies with the quality of the surface of the channels. Indeed, the quality of chips produced by laser ablation was more heterogeneous than that of chips prepared by hot embossing. The channels in the former chips did not fill simultaneously due to manufacturing defects like surface roughness, depth variation at channel connections, or material residues. Microfissures in the materials increased the fragility of chips produced by laser ablation, the bubble formation upon sample loading and sample dehydration. The properties of chips made by hot-embossing in PMMA and COC were the most satisfactory in terms of batch homogeneity and easiness of use for crystallization setup. Clean embossed channels also favor the growth of large mono crystals (see Fig. 5B) whereas rough relieves and material debris trigger heterogeneous nucleation and the growth of small crystals in channels produced by laser ablation.

Towards on-chip X-ray crystal analysis: When matter matters

On-chip crystal analysis was the ultimate goal of this project. Our first diffraction tests with the PDMS chip indicated that a 5 mm thick layer totally absorbs the incident X-ray beam. When the thickness of the polymer was reduced to ~1 mm and channels were

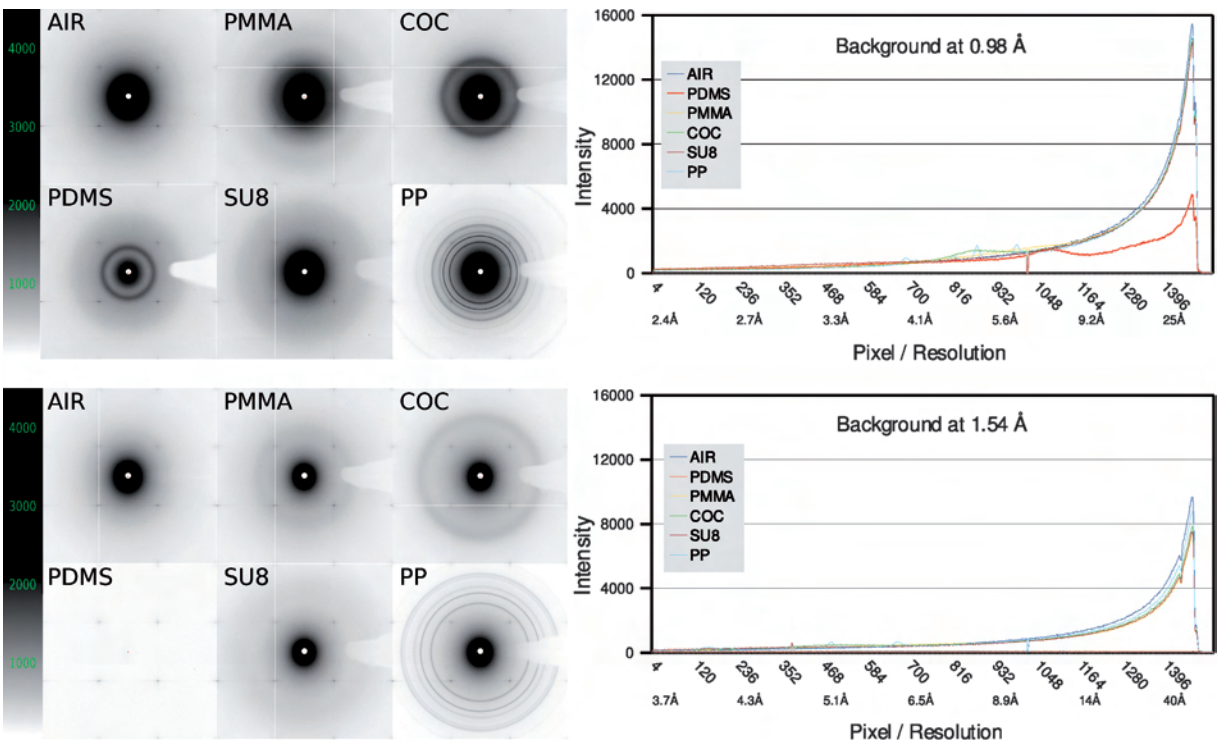

Fig. 4 Comparison of material X-ray scattering properties. This experiment compares the background image (30 sec exposure, 350 mm sample-to-detector distance) produced in the absence (*i.e.* in air only) and in the presence of some material in the X-ray beam. Scattered background signals were collected with an ADSC Quantum 315r detector which consists in a 3 × 3 array of CCD (charge-coupled device) modules. The active area is 315 × 315 mm^2 with 51 micron pixels in a 6144 grid. The images on the left hand side were collected at 0.98 Å (Top) and 1.54 Å (Bottom) in 2 × 2 binned mode and contained 3072 × 3072 pixels. The intensity of X-ray signal measured at each pixel site with a dynamic range of 16 bits (a value of 65536 corresponds to pixel saturation). The grayscale shown on the left is the same for all images. Corresponding radial profiles (pixels 1 to 1536 along the image x axis) are shown on the right hand side. Sample thickness (1 mm for PDMS and 230–250 μm for PMMA, COC, SU8 or PP) was chosen to be compatible with chip production. The background of thin materials does not differ significantly from that of air. In contrast, the background for PDMS is much lower at 0.98 Å and inexistent at 1.54 Å, revealing the strong direct beam attenuation due to material absorption.

sealed with a thin adhesive film (Fig. 3), the background scattering was much lower (Fig. 4) and diffraction patterns of a thaumatin crystal contained in a chip could be collected at room temperature. The limit of diffraction was modest (2.8 Å) because the material absorbs a great part of the direct beam and background scattering masks most of the weak reflections. Thus, in our opinion a chip made solely of PDMS is clearly not the best choice to collect high resolution diffraction data from biomolecule crystals. In spite of being very useful for fast prototyping, PDMS is too flexible at low thickness, generates parallax defects at high thickness and, for these reasons, makes an accurate alignment of the crystals in the X-ray beam difficult. Further, its permeability causes sample dehydration and its chemical composition is responsible for a strong absorption and scattering of X-rays.

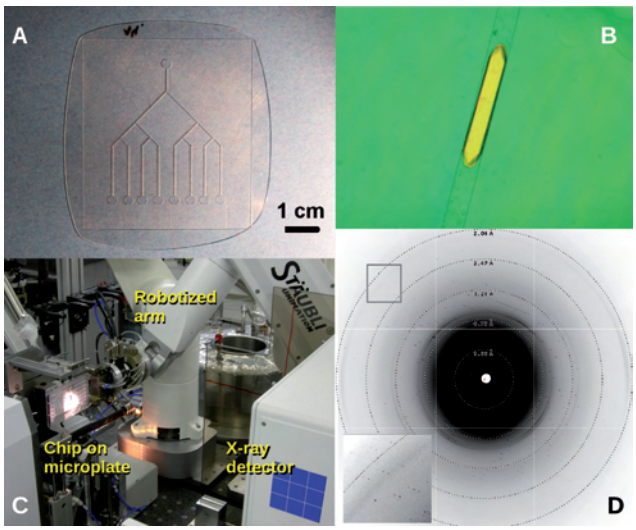

Fig. 5 On-chip crystal analysis at room temperature using synchrotron radiation. (A) Close-up view of a PMMA chip manufactured by hot embossing (thickness 250 μm). (b) Thaumatin crystal filling almost the entire crystallization channel. (C) Experimental setup on the FIP-BM30A beamline with a chip taped to a microplate hold in the beam by the arm of the robot.[23,24] (D) Diffraction pattern of a sample PMMA#1 (Table 1). The insert displays high resolution reflections in the boxed zone.

This prompted us to undertake a systematic comparison of the X-ray absorption and scattering properties of PDMS and of those of various light and rigid polymers, like PMMA, different types of COC, polypropylene or SU8 photoresist. Indeed, PMMA, polycarbonate or polyimide have recently been shown to be interesting alternatives.[41,42] Sheets of these materials with a thickness in conformity with the requirements of chip production (*i.e.* a thickness of 250 μm for rigid polymers and of 1 mm for PDMS) were placed in the incident beam of a synchrotron source (Fig. 4). The scattering backgrounds were measured at two wavelengths: 0.98 Å (corresponding to the selenium absorption edge used for structure phasing using the anomalous signal of selenomethionine-derivatized proteins) and 1.54 Å (produced by the copper anode of laboratory X-ray sources). The very low to null scattering signal measured with PDMS at both wavelengths clearly demonstrates that the high silicium content is not suitable for biomolecule crystals analysis by X-ray diffraction (Fig. 4). In contrast, all polymers containing only light atoms (C, O, N, H) exhibit scattering backgrounds that are comparable in intensity to that of air and this even at the highest wavelength. Polypropylene is the only material which shows discrete ring-like patterns characteristic of a micro-crystalline structure. In summary, the four polymers interfer much less with X-rays than PDMS and they are thus more compatible with the on-chip crystal characterization.

On the basis of these results, we selected PMMA and COC to manufacture new prototypes (Fig. 5). The better mechanical properties of these materials allow to reduce chip thickness by a factor 4 (*i.e.* down to 250 μm while a 1 mm layer of PDMS is very flexible and difficult to manipulate) while maintaining a good rigidity. As a consequence, the quality of the crystallographic data collected from crystals contained inside the chip was much improved (Table 1). Data collected on thaumatin crystals of the same age and size inside PDMS and PMMA chips can be directly compared. The lower diffraction limit (*i.e.* 2.8 Å with regard to 2 Å) and higher R*merge* values (*i.e.* lower agreement

Table 1 *On-chip* crystal analysis in different chip versions[a]

Chip version /crystal	PDMS	PMMA#1	PMMA#2	PMMA#3	COC#1	COC#2	COC
Protein	Thaumatin	Thaumatin	Thaumatin	Thaumatin	Thaumatin	Thaumatin	Lysozyme
Nb of images	20	40	40	40	114	124	62
Distance (mm)	300	300	300	300	250	250	300
Oscillation (s, degree)	2; 180	1; 30	1; 30	1; 20	0.5; 20	0.5; 30	1; 30
Space group	$P4_12_12$	$P4_12_12$	$P4_12_12$	$P4_12_12$	$P4_12_12$	$P4_12_12$	$P4_32_12$
Cell parameters a, c (Å)	58.3 151.6	58.4 151.6	58.4 151.5	58.5 151.7	58.6 151.5	58.6 151.4	79.1 37.9
Mosaicity (degree)	0.09	0.07	0.06	0.04	0.07	0.08	0.08
Resolution range (Å)	20–2.8	20–1.85	20–2.0	20–1.9	20–1.65	20–1.7	20–1.5
High resolution shell (Å)	2.97–2.8	1.96–1.85	2.12–2.0	2.01–1.9	1.75–1.65	1.8–1.7	1.6–1.5
No. observations	19494	63426	55386	61743	132297	136359	83112
No. unique reflections	5883	22357	17315	20044	29862	29362	18739
Completeness (%)	84.2 (87.3)	95.9 (86.5)	93.2 (94.3)	92.7 (89.0)	91.4 (88.5)	98 (97.2)	94.4 (83.7)
R*merge* (%)	12.9 (22.6)	5.7 (15.1)	11.6 (47.6)	10.4 (34.9)	10.2 (47.8)	10.7 (43.9)	6.6 (41)
I/σ(I)	9.0 (5.3)	13 (4.9)	8.0 (2.5)	8.7 (2.7)	8.9 (2.2)	9.6 (2.8)	13.4 (2.74)
Wilson plot B factor (Å^2)	22	23	27	24	27	24	24
Final R_{free} and R_{work}	0.29; 0.22	0.22; 0.18	0.24; 0.19	0.24; 0.20	0.25; 0.19	0.24; 0.19	0.16; 0.18
No. of water molecules	—	117	90	125	129	121	77

[a] Statistics for the high resolution shell are indicated between brackets.

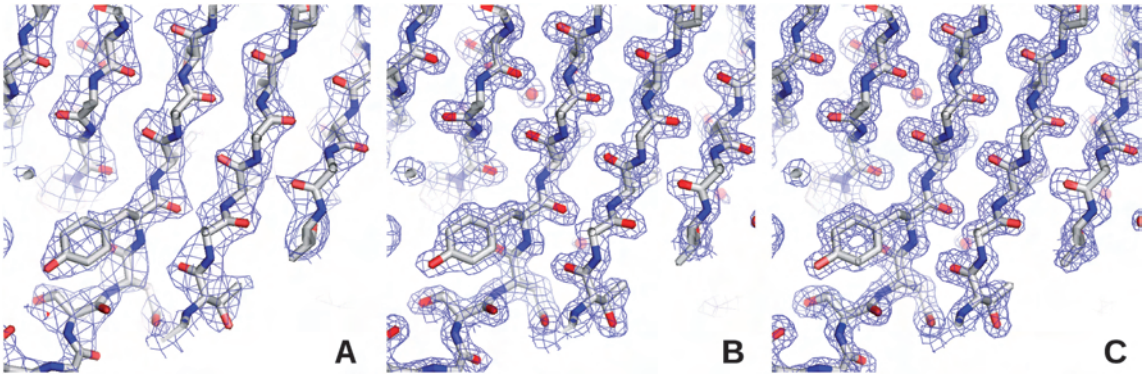

Fig. 6 Data collected in chips made of PMMA or COC lead to more detailed 3D structures. From left to right, same part of the $2F_o - F_c$ electron density maps derived from thaumatin crystals of similar volume analyzed in PDMS, PMMA#1 and COC#1. The maps contoured at 1.2 rms are at resolutions of 2.8, 1.85 and 1.65 Å, respectively. See data statistics given in Table 1.

between measurements of equivalent reflections) of the crystals inside PDMS are due to the stronger absorption of the incident and diffracted X-ray beam by this material. In contrast, crystals grown in PMMA chips (Fig. 6B) diffract X-rays beyond to 2 Å resolution, show better R*merge* statistics, even though the exposure times were 3 times shorter (30 s degree^{-1} instead of 90 s degree^{-1}). All thaumatin crystals display the same unit cell parameters, excellent crystal mosaicity values (<0.1°), as illustrated by the very sharp diffraction spots in the inset of Fig. 5D, and comparable B-factors (22–27 Å^2), indicating low molecular agitation in the crystal packing. This also stands for crystals of lysozyme and thaumatin grown in the presence of agarose gel in COC chips. In other words, the quality of all crystals is similar and differences in diffraction data are essentially due to the nature of chip material, PMMA and COC offering better thickness /absorption /rigidity compromise than PDMS. The quality of thaumatin crystals grown in COC chips cannot be directly compared to that observed in PMMA chips since the analysis was not carried out at the same time and in the same experimental conditions. In addition, the presence of agarose in the former might affect (improve) crystal diffraction properties.

Finally, our diffraction analyses demonstrate that preliminary crystal characterization, if not complete dataset measurements, can be carried out at room temperature *in situ*. The derived electron density maps (EDM) illustrate the quality of structural information that can be achieved (Fig. 6): data collected in PMMA and COC chips led to more detailed EDMs, and thus to improved 3D models, as indicated by better refinement statistics (lower R-factors) and an increased number of observable water molecules in the protein solvation shell.

5. Conclusion

We have demonstrated that the design we have chosen is suitable to produce simple and inexpensive microfluidic chips dedicated to the preparation of biomolecule crystals by CD. Our very first chips made of PDMS had the disadvantage to be too flexible for handling, insufficiently airtight to prevent dehydration during crystallization and not enough transparent to X-rays. Better performances were obtained with chips made of the thin and rigid polymers PMMA or COC that are transparent in visible light and X-rays. With these lab-on-a-chip prototypes, all steps of a structural genomics study from macromolecule to determination of its 3D structure could be performed.

Since on-chip crystal characterization is feasible, hazardous handling of crystals, *i.e.* the transfer in capillaries or nylon loops, is no longer necessary and best crystals can rapidly be identified at room temperature. In this way, each crystal will reveal its real diffraction potential. If cryo-cooling is required for the collection of full datasets, crystals can be extracted from the channels of the current set-up by removing the sealing film. However, room temperature data collection, which was the rule before the generalization of cryo-cooling, brings supplementary insights into biomolecule structure and dynamics in more realistic conditions. Presently, radiation damage occurring in a synchrotron beam is a major issue, but the situation may change in near future with the development of a new generation of detectors, for instance PILATUS detectors with ms readout times,[43] that enable continuous and much faster diffraction data collection.[43,44] The use of X-ray compatible chips and fast acquisition protocols that maximize data collection before severe crystal decay takes place will certainly contribute to the renaissance of crystallographic analyses at room temperature and provide valuable alternatives for samples that cannot by vitrified. In the present study, we have exploited a high crystal symmetry to reach near-to-complete data from single crystals despite some experimental constrains (sweep angle of the robotic arm <40°), but one can anticipate that the current developments on synchrotron facilities in automated sample handling, selection and analysis will soon provide convenient solutions for collecting and merging partial data from several low-symmetry crystals.

Finally, as mentioned above, crystals obtained in convection-free systems display better diffraction properties than those produced by conventional methods. Recently, an independent study using CD in microfluidic channels has confirmed this tendency.[32] Anyhow, CD chips open new opportunities for the fast, efficient and cost-effective growth of high quality crystals in miniaturized systems. Of course the application range of these chips is not at all restricted to biomolecules; it can easily be extended to small inorganic and organic compounds.

Acknowledgements

The authors thank the team of beamline FIP-BM30A at ESRF (Grenoble, France) for assistance during material and on-chip crystal characterization, as well as the MIMENTO technology platform at FEMTO-Innovation, the Centre National de la Recherche Scientifique (CNRS) for support in the frame of the Programme Interdisciplinaire de Recherche (PIR) 'Microfluidique et Microsystèmes Fluidiques', of the PNANO Programme from the Agence Nationale pour la Recherche (ANR) and the European Union (EU) Network of Excellence 'Multi-Material Micro Manufacture: Technologies and Applications (4M)' (FP6-500274-1). K.D. benefited from a joined BDI doctoral grant from CNRS and Région Alsace, G.T. from a grant in the framework of the EU thematic network 'NetMED: Virtual Institute on Micromechatronics for biomedical industry' (G7RT-CT-2002-05113) and C.S. was recipient of a Marie Curie European Reintegration Grant (MERG-CT-2004-004898).

References

1 A. Ducruix and R. Giegé, *Crystallization of nucleic acids and proteins: a practical approach* (second edition), IRL Press, Oxford, 1999.
2 R. Giegé and A. McPherson, Crystallizationgeneral methods, in *Crystallography Of Biological Macromolecules*, M. Rossmann and E. Arnold, Eds.; Kluwer Academic Publishers, Dordrecht, 2001; pp 81–110.
3 M. L. Pusey, Z. Liu, W. Tempel, J. Praissman, D. Lin, B. Wang, J. A. Gavira and J. D. Ng, Life in the fast lane for protein crystallization and X-ray crystallography, *Prog. Biophys. Mol. Biol.*, 2005, **88**, 359–386.
4 C. Hansen and S. R. Quake, Microfluidics in structural biology: smaller, faster. better, *Curr. Opin. Struct. Biol.*, 2003, **13**, 538–544.
5 F. Salemme, A free interface diffusion technique for crystallization of proteins for X-ray crystallography, *Arch. Biochem. Biophys.*, 1972, **151**, 533–540.
6 C. L. Hansen, E. Skordalakes, J. M. Berger and S. R. Quake, A robust and scalable microfluidic metering method that allows protein crystal growth by free interface diffusion, *Proc. Natl. Acad. Sci. USA*, 2002, **99**, 16531–16536.
7 C. L. Hansen, S. Classen, J. M. Berger and S. R. Quake, A microfluidic device for kinetic optimization of protein crystallization and *in situ* structure determination, *J. Am. Chem. Soc.*, 2006, **128**, 3142–3143.
8 M. J. Anderson, C. L. Hansen and S. R. Quake, Phase knowledge enables rational screens for protein crystallization, *Proc. Natl. Acad. Sci. USA*, 2006, **103**, 16746–16751.
9 B. Zheng, L. S. Roach and R. F. Ismagilov, Screening of protein crystallization conditions on a microfluidic chip using nanoliter-size droplets, *J. Am. Chem. Soc.*, 2003, **125**, 11170–11171.
10 B. Zheng, J. D. Tice, L. S. Roach and R. F. Ismagilov, A droplet-based, composite PDMS/glass capillary microfluidic system for evaluating protein crystallization conditions by microbatch and vapor-diffusion methods with on-chip X-ray diffraction, *Angew. Chem. Int. Ed. Engl.*, 2004, **43**, 2508–2511.
11 B. Zheng, C. J. Gerdts and R. F. Ismagilov, Using nanoliter plugs in microfluidics to facilitate and understand protein crystallization, *Curr. Opin. Struct. Biol.*, 2005, **15**, 548–555.
12 M. K. Yadav, C. J. Gerdts, R. Sanishvili, W. W. Smith, L. S. Roach, R. F. Ismagilov, P. Kuhn and R. C. Stevens, *In situ* data collection and structure refinement from microcapillary protein crystallization, *J. Applied Crystallogr.*, 2005, **38**, 900–905.
13 J. Shim, G. Cristobal, D. R. Link, T. Thorsen, Y. Jia, K. Piattelli and S. Fraden, Control and measurement of the phase behavior of aqueous solutions using microfluidics, *J. Am. Chem. Soc.*, 2007, **129**, 8825–8835.
14 J. M. García-Ruiz and A. Moreno, Investigations on protein crystal growth by the gel acupuncture method, *Acta Crystallogr. D Biol. Crystallogr.*, 1994, **50**, 484–490.
15 J. M. García-Ruiz, Counterdiffusion methods for macromolecular crystallization, *Meth. Enzymol.*, 2003, **368**, 130–154.
16 J. D. Ng, J. A. Gavira and J. M. García-Ruíz, Protein crystallization by capillary counterdiffusion for applied crystallographic structure determination, *J. Struct. Biol.*, 2003, **142**, 218–231.
17 J. A. Gavira, D. Toh, J. Lopéz-Jaramillo, J. M. García-Ruíz and J. D. Ng, *Ab initio* crystallographic structure determination of insulin from protein to electron density without crystal handling, *Acta Crystallogr. D Biol. Crystallogr.*, 2002, **58**, 1147–1154.
18 C. Sauter, B. Lorber, R. Giegé, A. Théobald-Dietrich, C. Khan Malek, B. Gauthier-Manuel, G. Thuillier and R. Ferrigno, Dispositif microfluidique pour la cristallisation et l'analyse cristallographique de molecules, *French patent application*, 19/07/2006,, *FR 06/06583*.
19 C. Sauter, K. Dhouib and B. Lorber, From macrofluidics to microfluidics for the crystallization of biological macromolecules, *Crystal Growth Design*, 2007, **7**, 2247–2250.
20 C. Khan Malek, G. Thuillier and P. Blind, Hybrid replication development for construction of polymeric devices, *J. Microsystem Technologies*, 2004, **10**, 711–715.
21 M. Sahli, C. Roques-Carmes, R. Duffait and C. Khan Malek, Study of the rheological properties of poly(methylmethacrylate) (PMMA) and cyclo-olefin-copolymer (COC) to optimize the hot-embossing process, In *Proc. 1st Int. Conf. on Multi-Material Micro Manufacture (4M)*, W. Menz and S. Dimov, Eds.; Elsevier, 2005; pp 71–74.
22 R. E. Matthews, Properties of nucleoprotein fractions isolated from turnip yellow mosaic virus preparations, *Virology*, 1960, **12**, 521–539.
23 L. Jacquamet, J. Ohana, J. Joly, F. Borel, M. Pirocchi, P. Charrault, A. Bertoni, P. Israel-Gouy, P. Carpentier, F. Kozielski, D. Blot and J. Ferrer, Automated analysis of vapor diffusion crystallization drops with an X-ray beam, *Structure*, 2004, **12**, 1219–1225.
24 L. Jacquamet, J. Ohana, J. Joly, P. Legrand, R. Kahn, F. Borel, M. Pirocchi, P. Charrault, P. Carpentier and J. L. Ferrer, A new highly integrated sample environment for protein crystallography, *Acta Crystallogr. D Biol. Crystallogr.*, 2004, **60**, 888–894.
25 W. Kabsch, XDS, in *International Tables for Crystallography, Vol. F. Crystallography of Biological Macromolecules*, M. G. Rossmann and E. Arnold, Eds.; Kluwer Academic Publishers, Dordrecht, 2001; pp 730–734.
26 Collaborative Computational Project Number 4, The ccp4 suite: programs for protein crystallography, *Acta Crystallogr. D Biol. Crystallogr.*, 1994, **50**, 760–763.
27 P. D. Adams, R. W. Grosse-Kunstleve, L. W. Hung, T. R. Ioerger, A. J. McCoy, N. W. Moriarty, R. J. Read, J. C. Sacchettini, N. K. Sauter and T. C. Terwilliger, PHENIX: building new software for automated crystallographic structure determination, *Acta Crystallogr. D Biol. Crystallogr.*, 2002, **58**, 1948–1954.
28 A. Vergara, B. Lorber, C. Sauter, R. Giegé and A. Zagari, Lessons from crystals grown in the advanced protein crystallisation facility for conventional crystallisation applied to structural biology, *Biophys. Chem.*, 2005, **118**, 102–112.
29 B. Lorber, C. Sauter, J. D. Ng, D. W. Zhu, R. Giegé, O. Vidal, M. C. Robert and B. Capelle, Characterization of protein and virus crystals by quasi-planar wave X-ray topography: a comparison between crystals grown in solution and in agarose gel, *J. Crystal Growth*, 1999, **204**, 357–368.
30 F. J. López-Jaramillo, J. M. García-Ruiz, J. A. Gavira and F. Otálora, Crystallization and cryocrystallography inside X-ray capillaries, *J. Applied Crystallog.*, 2001, **34**, 365–370.
31 J. M. García-Ruiz, F. Otálora, M. Novella, J. Gavira, C. Sauter and O. Vidal, A supersaturation wave of protein crystallization, *J. Crystal Growth*, 2001, **232**, 149–155.
32 J. D. Ng, P. J. Clark, R. C. Stevens and P. Kuhn, *In situ* X-ray analysis of protein crystals in low-birefringent and X-ray transmissive plastic microchannels, *Acta Crystallogr. D Biol. Crystallogr.*, 2008, **64**, 189–197.
33 J. J. Brandner, W. Pfleging, T. Gietzelt, T. Henning, M. Kraut and H. Moritz, Microfabrication in metals and polymers, *Advanced Micro and Nano Systems*, 2006, **5**, 267–319.
34 C. Khan Malek, Laser processing for bio-microfluidics applications (part i), *Anal. Bioanal. Chem.*, 2006, **385**, 1351–1361.
35 C. Khan Malek, Laser processing for bio-microfluidics applications (part ii), *Anal. Bioanal. Chem.*, 2006, **385**, 1362–1369.

36 W. Pfleging, M. Przybylski and H. J. Brückner, Excimer laser material processing – state of the art and new approaches in microsystem technology, *SPIE*, 2006, **6107**, 61070G-1-15.
37 W. Pfleging, P. Schierjott and C. Khan Malek, Rapid fabrication of functional pmma microfluidic devices by CO_2-laser patterning and hpd-laser transmission welding, in *Laser Assisted Net Shape Engineering 5*, Vol. 2, M. Geiger, A. Otto and M. Schmidt, Eds.; Meisenbach-Verlag, Bamberg, 2007; pp 1207–1220.
38 W. Pfleging, W. Bernauer, T. Hanemann and M. Torge, Rapid fabrication of microcomponents - UV-laser assisted prototyping, laser micro-machining of mold inserts and replication *via* photomolding, *Microsystem Technologies*, 2002, **9**, 67–74.
39 W. Pfleging, T. Hanemann, M. Torge and W. Bernauer, Rapid fabrication and replication of metal, ceramic and plastic mold inserts for application in microsystem technologies, *J. Mechanical Engineering Science*, 2003, **217**, 53–63.
40 A. McPherson, S. Koszelak, H. Axelrod, J. Day, R. Williams, L. Robinson, M. McGrath and D. Cascio, An experiment regarding crystallization of soluble proteins in the presence of beta-octyl glucoside, *J. Biol. Chem.*, 1986, **261**, 1969–1975.
41 E. D. Greaves and A. Manz, Towards on-chip X-ray analysis, *Lab Chip*, 2005, **5**, 382–391.
42 R. Barrett, M. Faucon, J. Lopez, G. Cristobal, F. Destremaut, A. Dodge, P. Guillot, P. Laval, C. Masselon and J. Salmon, X-ray microfocussing combined with microfluidics for on-chip X-ray scattering measurements, *Lab Chip*, 2006, **6**, 494–499.
43 C. Broennimann, E. F. Eikenberry, B. Henrich, R. Horisberger, G. Huelsen, E. Pohl, B. Schmitt, C. Schulze-Briese, M. Suzuki, T. Tomizaki, H. Toyokawa and A. Wagner, The PILATUS 1M detector, *J. Synchrotron Radiation*, 2006, **13**, 120–130.
44 R. J. C. Hilf and R. Dutzler, X-ray structure of a prokaryotic pentameric ligand-gated ion channel, *Nature*, 2008, **452**, 375–379.
45 B. Lorber, J. B. Bishop and L. J. DeLucas, Purification of octyl β-D-glucopyranoside and re-estimation of its micellar size, *Biochim. Biophys. Acta*, 1990, **1023**, 254–265.